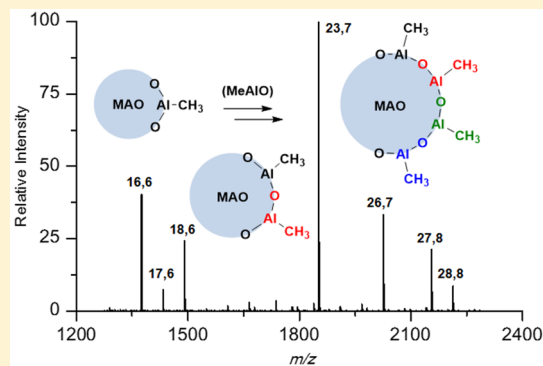


## Additive and Aging Effects on Methylalumoxane Oligomers

Harmen S. Zijlstra,<sup>†</sup> Mikko Linnolahti,<sup>‡</sup> Scott Collins,<sup>†</sup> and J. Scott McIndoe<sup>\*,†</sup><sup>†</sup>Department of Chemistry, University of Victoria, P.O. Box 3065, Victoria, British Columbia V8W 3V6, Canada<sup>‡</sup>Department of Chemistry, University of Eastern Finland, P.O. Box 111, FI-80101 Joensuu, Finland

## Supporting Information

**ABSTRACT:** In the presence of the weak donor octamethyltrisiloxane (OMTS), methylalumoxane (MAO) undergoes ionization through  $[\text{Me}_2\text{Al}]^+$  abstraction. The  $[\text{Me}_2\text{Al}\cdot\text{OMTS}]^+[(\text{MeAlO})_x(\text{Me}_3\text{Al})_y\text{Me}]^-$  ion pairs formed can conveniently be studied by electrospray ionization mass spectrometry. The anion distribution changes with OMTS:Al ratio, with low molecular weight (MW) anions forming at high ratios due to oligomer degradation. Monitoring of room-temperature aging shows that MAO oligomers of low MW are slowly and systematically converted to species with higher MW through addition of (MeAlO) units, and intermediate oligomers are observed and assigned. This process occurs at room temperature but does not occur significantly over a period of months at low temperatures. Computational investigations of these species show large cage-like clusters with four-coordinate Al and three-coordinate O. All neutral structures have sites that could readily give up  $[\text{Me}_2\text{Al}]^+$  to form the observed ions, though sites that can lose  $[\text{Me}_2\text{Al}]^+$  without leaving a two-coordinate oxygen site are favored. These studies provide concrete insights into the absolute MW of MAO oligomers and their exchange over time.



These studies provide concrete insights into the absolute MW of MAO oligomers and their exchange over time.

## INTRODUCTION

The serendipitous discovery of the activating powers of methylalumoxane (MAO)<sup>1</sup> has allowed for the development and commercialization of homogeneous single-site polymerization catalysts.<sup>2</sup> MAO is widely used as a cocatalyst, transforming precatalysts by alkylation and ionization. Its different roles in these processes have been studied in detail and are relatively well understood.<sup>3</sup> The structure and detailed working principles of MAO, however, remain unclear.<sup>4</sup> MAO is produced by the controlled, partial hydrolysis of trimethylaluminum ( $\text{Me}_3\text{Al}$ ), providing MAO oligomers and residual  $\text{Me}_3\text{Al}$  that are in dynamic equilibrium. This complex mixture varies with time and temperature, making it very hard to characterize. Over the past decades many studies have been carried out to give a general idea of the structure of MAO. Its average composition,  $(\text{Me}_{1.4-1.5}\text{AlO}_{0.75-0.80})_n$ <sup>5</sup> has been established, and several characteristics such as coordination number of Al (mainly 4) and O (3),<sup>6</sup> average molecular weight (MW, 1200–2000), and degree of polymerization ( $n = 20-30$ )<sup>7</sup> are generally agreed upon. On the basis of these findings, calculations,<sup>8</sup> and the established geometries of related alumoxanes,<sup>9</sup> different structures have been proposed for MAO.<sup>4</sup> The consensus of all this work is that MAO is comprised largely of cage-like structures that have the general formula  $(\text{MeAlO})_n(\text{Me}_3\text{Al})_m$ , where a large number of different oligomers are expected to be stable.

In order to gain concrete insight into the different oligomers present in MAO solution, it is desirable to establish the absolute molecular weight of the different species present. Upon ionization of MAO, electrospray ionization mass

spectrometry (ESI-MS) can be used to detect individual ions. This technique has been used to study metallocenium ions in olefin polymerization, but its use to study MAO has been limited.<sup>10</sup> ESI-MS provides indirect information about the composition of MAO itself, as it only detects ions and does not see neutrals. Initial ESI-MS studies led to decomposition of the highly air and moisture sensitive MAO.<sup>11</sup> We found that oxidation and hydrolysis can be overcome by the use of a glovebox<sup>12</sup> in combination with scrupulously dried fluorobenzene (PhF).<sup>13</sup> Negative and positive ion studies using MAO purchased from Sigma-Aldrich and  $\text{Cp}_2\text{ZrX}_2$  ( $X = \text{Cl}, \text{Me}$ ), octamethyltrisiloxane (OMTS), or  $[\text{nBu}_4\text{N}]^+\text{Cl}^-$  as additive led to the formation of ion pairs with the general formula  $[\text{M}]^+[(\text{MeAlO})_x(\text{Me}_3\text{Al})_y\text{Me}]^-$  (where  $[\text{M}]^+ = [\text{Cp}_2\text{Zr}(\mu\text{-X}_2)\text{AlMe}_2]^+$ ,  $[\text{Me}_2\text{Al}\cdot\text{OMTS}]^+$ ,  $[\text{nBu}_4\text{N}]^+$ ).<sup>14</sup> The formation of these ions can all be rationalized by neutral MAO entities giving up  $[\text{Me}_2\text{Al}]^+$  to produce MAO anions. These findings support the idea that MAO may act as a source of  $[\text{Me}_2\text{Al}]^+$  during catalyst activation.<sup>15,16</sup> The charged species observed give an indirect indication of the neutral composition, as they show the oligomers in neutral MAO that are ionized.

In this paper, we present systematic studies of the effect of the OMTS:Al ratio on anion speciation and an in-depth study of MAO aging, enabled by improvements in our methodologies. We focused exclusively on OMTS, as it is air-stable, is not hygroscopic, reacts with MAO to give the single cation  $[\text{Me}_2\text{Al}\cdot\text{OMTS}]^+$ , and provides negative ion spectra with higher

Received: February 27, 2017

Published: April 25, 2017

intensity in comparison with  $\text{Cp}_2\text{ZrMe}_2$ . Anion formation and stability are examined with complementary theoretical techniques that shed light on the generation of anions from neutral precursors and their respective structures.

## RESULTS AND DISCUSSION

**ESI-MS Investigation.** Sigma-Aldrich stopped selling MAO solutions in 2014; therefore, a sample supplied by Albemarle as a 10 wt % solution was used for this work. This material, as received, was analyzed by NMR spectroscopy following literature procedures and found to contain 13–14 mol % of  $\text{Me}_3\text{Al}$  and 1.0 mol % of  $[\text{Me}_2\text{Al}]^+$ .<sup>5,16</sup> The  $\text{Me}_3\text{Al}$  value is fairly similar to that of the MAO solutions supplied by Sigma-Aldrich, whereas the amount of the cationic activator is approximately twice as high. We have stored and used this material for over 2 years, and the  $\text{Me}_3\text{Al}$  content was little changed, while there was a modest decline in the amount of  $[\text{Me}_2\text{Al}]^+$  to 0.7 mol %.

Comparison of the negative ESI-MS data from the Albemarle sample with the previously obtained sample from Sigma-Aldrich<sup>14a</sup> shows distinct differences (Figure 1). Upon addition

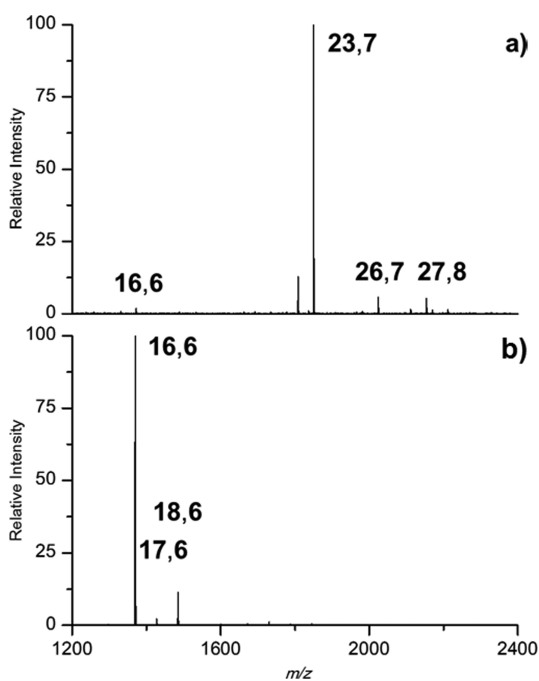


**Figure 1.** Comparison of negative ion ESI-MS in PhF of (a) Sigma-Aldrich<sup>14a</sup> and (b) Albemarle samples of 10 wt % MAO with an OMTS:Al ratio of 1:100.

of OMTS to MAO in a 1:100 ratio with respect to the total [Al] (OMTS:Al; 10 wt % of MAO is approximately 1.5 M in Al) the negative ion spectra are overwhelmingly dominated by a single anion with the composition  $[(\text{MeAlO})_{16}(\text{Me}_3\text{Al})_6\text{Me}]^-$  (Figure 1b), whereas in the earlier reports using Sigma-Aldrich MAO the negative spectra were dominated by the higher MW anion  $[(\text{MeAlO})_{23}(\text{Me}_3\text{Al})_7\text{Me}]^-$  (Figure 1a).<sup>14a</sup> Henceforth, we will describe all species by the notation  $x,y$  based on the empirical formula  $[(\text{MeAlO})_x(\text{Me}_3\text{Al})_y\text{Me}]^-$ : for example,  $[(\text{MeAlO})_{16}(\text{Me}_3\text{Al})_6\text{Me}]^-$  will simply be 16,6. This notation carries limited structural implication but allows us to abbreviate all observed ions.

Closer analysis shows that all ions observed in the Albemarle sample can also be found in the spectrum of the Sigma-Aldrich

sample. Additionally, the Sigma-Aldrich sample contained several anions not observed in the Albemarle sample, most notably being the ion with  $m/z$  1811, 42 Da lower in mass than 23,7.

The second and third most intense anions in the Albemarle spectrum can be assigned to 17,6 and 18,6, respectively, in Figure 1b. These ions differ in mass by one or two (MeAlO) units (58 Da) with respect to the most intense ion. This suggests that these anions are closely related to each other. This observation is supported by MS/MS product ion spectra, which show that all ions lose the same number of  $\text{Me}_3\text{Al}$  molecules (see the Supporting Information). Additional ions of minor intensity show up at higher mass (vide infra), indicating that a variety of different, neutral MAO precursors can be ionized.

Due to the low degree of ionization, these higher MW ions are not of sufficient intensity to study in detail. In an attempt to boost their intensity, we investigated the effect of the OMTS:Al ratio on the negative ion spectrum. If the ratio is decreased from 1:100 to 1:500, only the 16,6 ion is observed, meaning that its neutral precursor is the MAO component that most readily ionizes (Figure 2a).

If, instead, the ratio of OMTS:Al is increased from 1:100 to 1:50, ions with the formulas 17,6 and 18,6 increase in intensity in comparison to 16,6 (Figure 2b). A small amount of a new low-molecular-weight ion assignable as 12,5 appears. This anion is most likely formed upon degradation of higher mass compounds, which is in accordance with earlier work that showed the average MW of MAO to decrease significantly in the presence of large amounts of donors.<sup>7a</sup> The increase in low-MW anions is continued when the OMTS:Al ratio is further increased to 1:10 and 1:1 (Figure 2c,d). The intensity of the 12,5 ion increases further, and the ions 10,4, 10,5, and 11,5 appear while the intensities of the ions 17,6 and 18,6 do not increase relative to the main 16,6 signal. As in the 1:100 spectrum (Figure 1b), all observable anions can be related to each other by addition or subtraction of (MeAlO) and/or  $\text{Me}_3\text{Al}$  units.

At an OMTS:Al ratio of 1:1 enough ions are generated through ionization of MAO that the spectral quality is significantly improved. This is consistent with previous observations which showed that, in order to obtain good ESI mass spectra in solvents of relatively low polarity, a supporting electrolyte can be added to boost the signal to noise ratio.<sup>17</sup> As the signal to noise ratios are excellent good-quality data on the minor ions observed at molecular weights >1500 could be collected. A series of signals that are all systematically related by (MeAlO) and  $\text{Me}_3\text{Al}$  units is seen (Figure 3).

At least three series of MAO anions can be distinguished (red, green, and blue). The species within each series vary in (MeAlO) units, whereas the anions from one series to another vary by ( $\text{Me}_3\text{Al}$ ) units. The higher the  $x$  value of a series (i.e., the higher the degree of oligomerization), the more likely this series is to contain an additional  $\text{Me}_3\text{Al}$  molecule. Almost no oligomers of series where  $y < 6$  are seen (see Figure S2 in the Supporting Information). An increase in the number of (MeAlO) units eventually leads to a high enough increase in surface area that another molecule of  $\text{Me}_3\text{Al}$  can be incorporated. These series are systematic and may be indicative of the interconversion of low-MW species such as the neutral precursor of 16,6 into the precursor of the higher MW species such as 23,7 in MAO solutions.

In our hands the negative ion spectra of the MAO samples showed very little change in anion distribution over time when

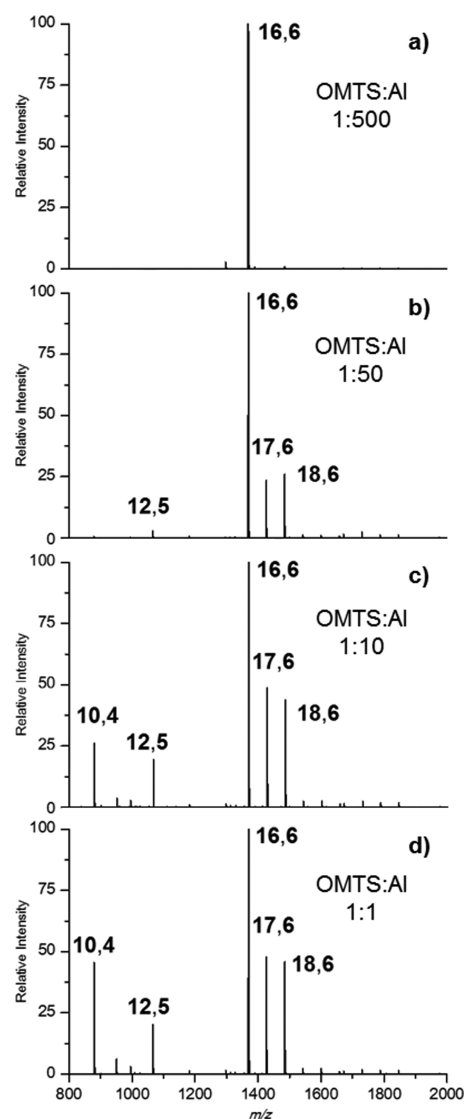


**Figure 2.** Comparison of negative ion ESI-MS in PhF of an Albemarle sample of 10 wt % MAO with varying OMTS:Al ratios: (a) 1:500; (b) 1:50; (c) 1:10; (d) 1:1.

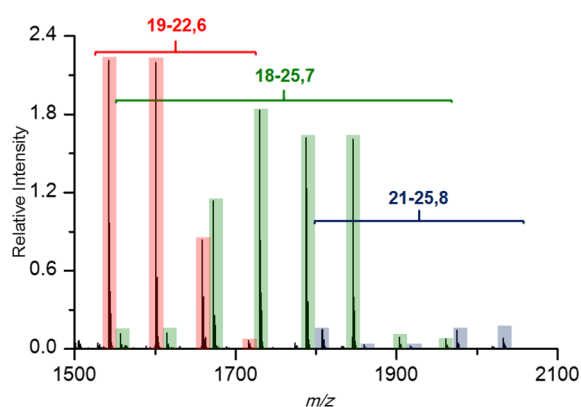


**Figure 3.** Negative ion ESI-MS in PhF of an Albemarle sample of 10 wt % MAO with an OMTS:Al ratio of 1:1.

samples were stored in the freezer over the course of 2 years (vide supra). To investigate the effect of storage on anion distribution, we obtained another sample of Albemarle MAO

that had been stored in a steel cylinder at room temperature inside a glovebox for 11 months (Figure 4).

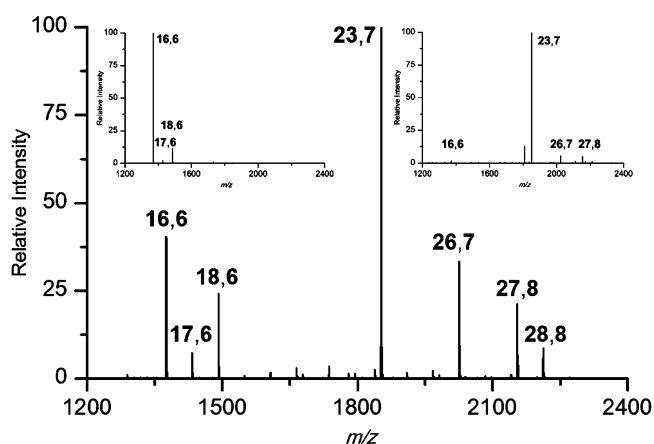
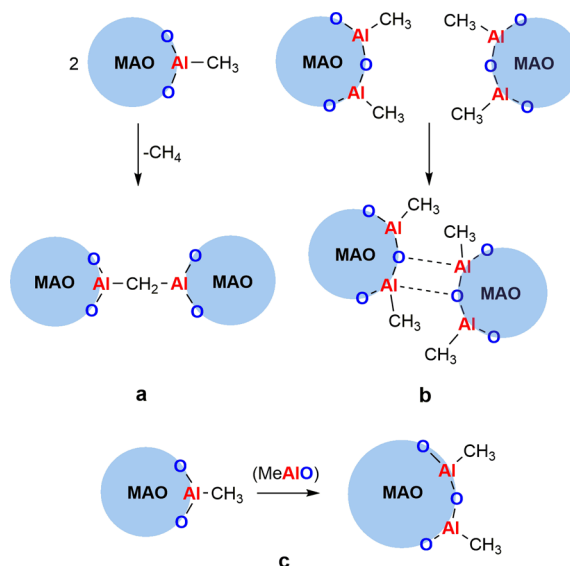


**Figure 4.** Negative ion spectra of an 11 month old sample of Albemarle 10 wt % MAO stored at room temperature with an OMTS:Al ratio of 1:100. Insets: (top left) Albemarle sample stored at  $-20\text{ }^{\circ}\text{C}$ ; (top right) Sigma-Aldrich sample.

The appearance of this spectrum is intermediate between the Sigma Aldrich and Albemarle samples shown before (see Figure 1). The 16,6 ion and the derivatives containing one and two more (MeAlO) units are still present, but the 23,7 ion has now become the most intense anion, while higher MW oligomers are also observed. This change in the anion distribution may be explained by slow conversion of low-MW MAO oligomers to higher-MW oligomers through addition of (MeAlO) units over time.

MAO solutions are known to form higher molecular weight material upon aging, eventually resulting in the precipitation of a gel. Previous studies have suggested that this aging could take place through reversible and irreversible self-condensation<sup>18</sup> (Scheme 1a,b), but addition of (MeAlO) units over time has not previously been observed to the best of our knowledge.

**Scheme 1.** MAO MW Increase through Chemically Irreversible (a) and Physically Reversible (b) Self-Condensation and Addition of (MeAlO) Units (c)



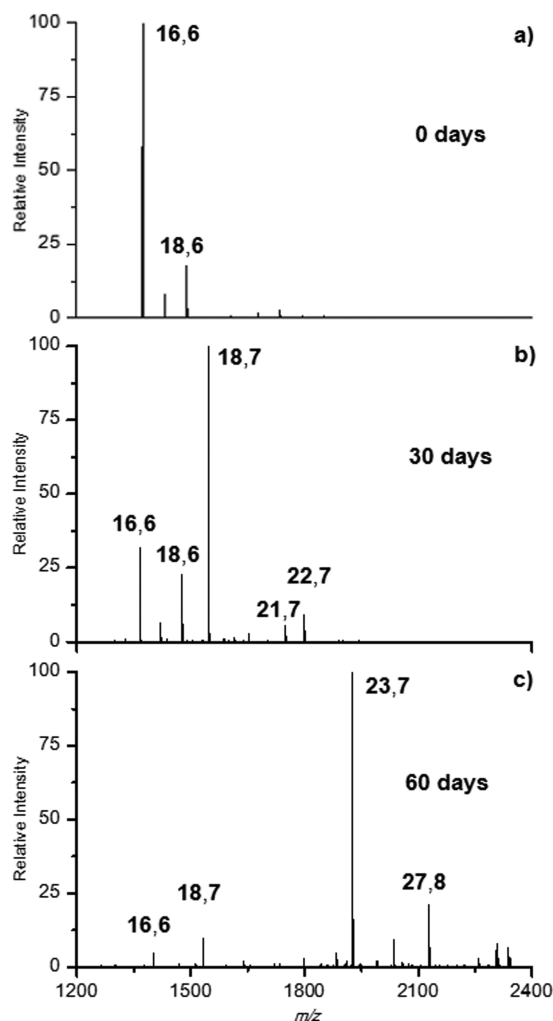
Self-condensation would form MAO aggregates with a MW higher than any that we observe by ESI-MS. For example, if two molecules of  $(\text{MeAlO})_{16}(\text{Me}_3\text{Al})_7$ , a possible precursor to **16,6**, undergo the reaction in Scheme 1a, they would condense to form  $[(\text{Me}_3\text{Al})_7(\text{MeAlO})_{15}(-\text{OAl}-\mu-\text{CH}_2-\text{AlO}-)(\text{MeAlO})_{15}(\text{Me}_3\text{Al})_7]$ . If this precursor were to ionize through  $[\text{Me}_2\text{Al}]^+$  abstraction, the ion formed would have the formula  $[(\text{MeAlO})_{30}(-\text{OAl}-\mu-\text{CH}_2-\text{AlO}-)(\text{Me}_3\text{Al})_{13}\text{Me}]^-$  and appear at  $m/z$  2791. We did not see this anion in any of our spectra. Insoluble species are also not tractable by ESI-MS; thus, the fact that we do not observe such species by mass spectrometry does not mean that they are not forming. Indeed, such gels visibly form over the time scale of the aging experiments and the total ion intensity for the aged samples is much less than that for the samples stored in the freezer. Additionally, it is also quite possible that such massive MAO oligomers are less prone to release  $[\text{Me}_2\text{Al}]^+$ , making them undetectable to ESI-MS (as well as less significant as activators). Although we cannot exclude other aging processes that increase MW, we can observe that slow, regular increases in the degree of oligomerization are definitely occurring in MAO samples as they age (see Scheme 1c).

To further study the aging process, we deliberately accelerated the aging of a MAO sample. A solution of Albemarle MAO from the freezer was analyzed and stored in a glass vial inside the glovebox. Its composition was monitored over time, and a clear change in ion distribution was observed (Figure 5).

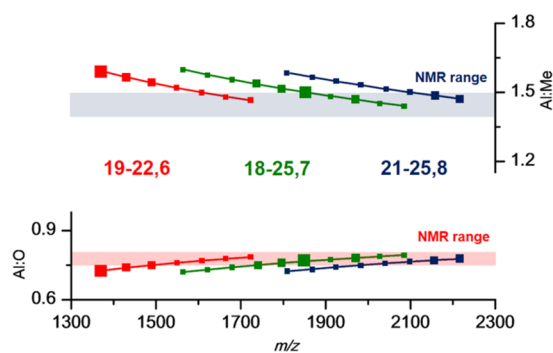
The relative intensity of the high-MW anions increases over time, and at 60 days the sample shows remarkable similarities to Sigma-Aldrich samples (see Figure 1). The shift from predominantly low-MW ions to high-MW ions goes through various other MAO oligomers, slowly increasing in size by addition of  $(\text{MeAlO})$  and  $\text{Me}_3\text{Al}$  over time. It should be noted that the increase in high-MW anions for the samples stored in the glass vials is much more rapid than that of the Albemarle sample aged in a steel cylinder. This can be attributed to the storage conditions: a steel cylinder protects from external perturbations (e.g., water, oxygen, light) more effectively than a capped vial.

Through combination of all anions observed under all conditions, trends can be seen. The different MAO series increase in  $(\text{MeAlO})$  units until they become large enough to attract an additional molecule of  $\text{Me}_3\text{Al}$  to its surface. At this point the next higher series starts to become predominant (Figure 6). Upon an increase in the number of  $(\text{MeAlO})$  units the Al:O ratio goes up while the Al:Me ratio goes down. Initially the overall Me:Al:O ratios are outside of the range established by NMR, but as the MW increases, they fit well with the established values.<sup>5</sup> The MW range at which the Me:Al:O ratio matches that reported in the literature is also the range in which the average MW has previously been described,<sup>7</sup> indicating that the data obtained by ESI-MS are in good agreement with literature reports.

While the ESI-MS results concur with the NMR data, the former necessarily only probe the anionic species generated through reaction of OMTS to form  $[\text{Me}_2\text{Al}\cdot\text{OMTS}]^+[(\text{MeAlO})_x(\text{Me}_3\text{Al})_y\text{Me}]^-$ . The neutral precursors of these ion pairs are not necessarily representative of the entire ensemble; rather, the ESI-MS observation of an anion does point to the existence of a corresponding reactive neutral species. The MW information so obtained can be used to fine-tune computational efforts into the structure of the “active



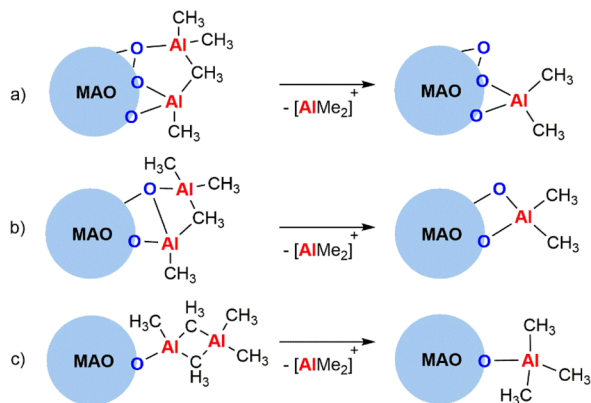
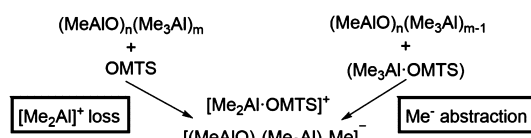
**Figure 5.** Negative ion mass spectra of a sample of Albemarle 10 wt % MAO with an OMTS:Al ratio of 1:100 (a) from the freezer and (b) after 30 days and (c) after 60 days of storage at room temperature.



**Figure 6.** Plots of Al:O and Al:Me ratios of all  $[\text{MAO-Me}]^-$  ions observed. Larger squares indicate major species; smaller squares indicate minor species (<5% of the base peak in all spectra collected).

ingredient(s)” of MAO. Accordingly, the major anions and their neutral precursors were studied using DFT methods.

**DFT Calculations.** In previous work, we computationally studied hydrolysis reactions of  $\text{Me}_3\text{Al}$  that produced models of small MAO oligomers of the general formula  $(\text{MeAlO})_n(\text{Me}_3\text{Al})_m$  with  $n = 1-8$  and  $m = 0-5$ .<sup>8b,14b,19b</sup> To produce representative models for the higher MW oligomers observed

Scheme 2. Potential MAO Sites That Could Lose  $[\text{Me}_2\text{Al}]^+$ Scheme 3. Possible Routes to  $[\text{Me}_2\text{Al}\cdot\text{OMTS}]^+[(\text{MeAlO})_x(\text{Me}_3\text{Al})_y\text{Me}]^-$  from a Combination of OMTS with Neutral Precursors

during the ESI-MS work, we continued the systematic exploration of the hydrolysis reactions to reach neutral MAO oligomers with  $m$  and  $n$  values varying from 16 to 26 and from 6 to 8, respectively. In accordance with previous computational studies<sup>8,19,20</sup> all MAO oligomers were found to be primarily formed of an  $(\text{MeAlO})_n$  core with four-coordinate Al and three-coordinate O atoms. Association of  $\text{Me}_3\text{Al}$  into the  $(\text{MeAlO})_n$  core creates sites composed of four-coordinate oxygen and/or methyl bridges between adjacent Al atoms, and both motifs are reactive. Indeed, all neutral MAO oligomers possess multiple reactive sites which could potentially give up  $[\text{Me}_2\text{Al}]^+$ . We transformed these neutral species into anions by removal of  $[\text{Me}_2\text{Al}]^+$  from feasible sites of the MAOs. The relative anionization potentials of the different  $[\text{Me}_2\text{Al}]^+$  losses were compared, and the most stable structures resulting from this process for the major ions observed (16,6, 17,6, 18,6, 23,7, and 26,7) are given in Table 1.

In this discussion, we will focus primarily on  $n,m = 16,7$ , as it is this neutral oligomer that could generate the 16,6 ion prominent in the mass spectrometric analysis of fresh Albemarle MAO solutions (Figure 1b). It also displays behavior that is largely representative of the higher MW oligomers. The calculated model structure of  $(\text{MeAlO})_{16}(\text{Me}_3\text{Al})_7$  has various sites that could lose  $[\text{Me}_2\text{Al}]^+$ , and the relative differences in ionization energies were calculated (Scheme 2).

The ionization energies through  $[\text{Me}_2\text{Al}]^+$  loss of all bonding environments shown in Scheme 2 were calculated. It was found that for  $(\text{MeAlO})_{16}(\text{Me}_3\text{Al})_7$  pathway c in Scheme 2c ( $-125.1$  to  $-132.8$  kJ/mol) was preferred over pathways a and b ( $-2.1$  to  $-43.4$  kJ/mol). The reasons behind the difference in the site propensity for  $[\text{Me}_2\text{Al}]^+$  loss may be rationalized. The site(s) most willing to give up  $[\text{Me}_2\text{Al}]^+$  have  $\text{Me}_2\text{Al}$  fragments bound via two bridging methyl groups, and when it departs the oligomer as  $[\text{Me}_2\text{Al}]^+$ , it leaves an  $\text{Me}_3\text{Al}$  bound terminally to a three-coordinate oxygen. Pathways which have  $\text{Me}_2\text{Al}$  bound to oxygen atoms leave two-coordinate oxygen atoms upon

departure, and such transformations are much less favorable energetically and have not been experimentally observed.

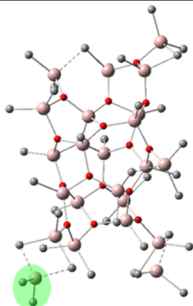
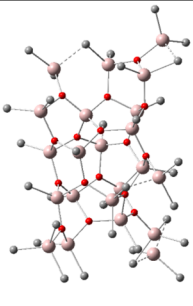
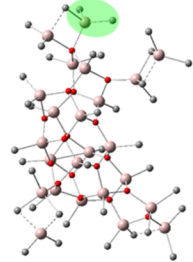
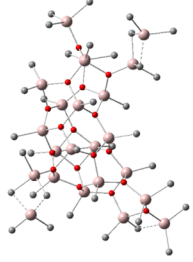
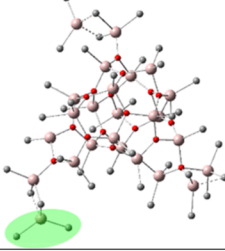
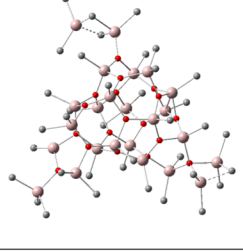
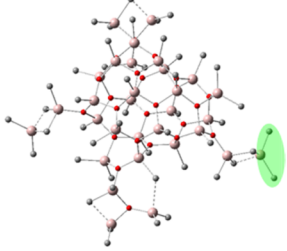
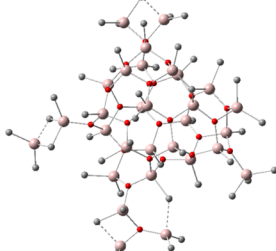
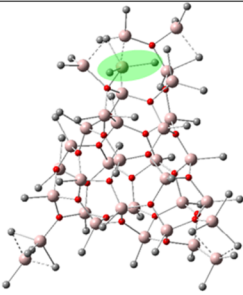
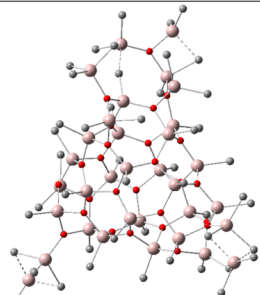
Formation of 16,6, the most abundant ion in our MS spectra, has the least favorable anionization potential of all calculated MAO oligomers (see Table 1). This might suggest that its precursor has a high abundance in the neutral MAO mixture. Systematic computational investigation to shed light on the distribution of the neutral MAOs is in progress. The processes being compared involve the same kind of structural unit,  $(\mu_3\text{-O})\text{Al}_2\text{Me}_5$ , as well as the lowest energy pathway (Scheme 2c); therefore, the comparison is internally consistent and should not be strongly perturbed by ground state energy differences. An alternate possibility for ion pair formation is that a donor–acceptor complex between OMTS and the most abundant Lewis acid present (i.e.,  $\text{Me}_3\text{Al}$ ) undergoes methide abstraction to yield the same ion pairs (Scheme 3).

We have examined both processes for a number of the anions formed. For the 16,6 anion, formation of the most stable anion with  $m/z$  1375 involves  $\text{Me}^-$  abstraction from a precursor with MW 1360. This process is favored by 40.9 kJ/mol over  $\text{Me}_2\text{Al}^+$  abstraction from a precursor with MW 1432. On the other hand, both pathways are equal in energy for formation of 16,7 while  $[\text{Me}_2\text{Al}]^+$  abstraction is favored by 10.5 kJ/mol for 16,8. The nature of the additive, its interaction with “free”  $\text{Me}_3\text{Al}$  vs MAO, and its ability to stabilize the highly reactive  $[\text{Me}_2\text{Al}]^+$  will influence the energy of either pathway and may account for difference in predicted vs observed anion distributions. More detailed and complete studies investigating a series of neutral MAO oligomers, their relative stabilities, ionization energies (through  $[\text{Me}_2\text{Al}]^+$  loss vs  $\text{Me}^-$  abstraction), and the influence of the additive on the respective energies is currently ongoing and will be reported in due course.

## CONCLUSIONS

In the presence of the bidentate donor OMTS, MAO easily ionizes to form  $[\text{Me}_2\text{Al}\cdot\text{OMTS}]^+[(\text{MeAlO})_x(\text{Me}_3\text{Al})_y\text{Me}]^-$  ion pairs. The negative ion distribution obtained from a sample purchased directly from Albemarle was remarkably different from that in earlier reports using Sigma-Aldrich samples. Detailed ESI-MS studies show that this is due to aging of samples at room temperature prior to shipping. The anion distribution changes with OMTS:Al ratio, with low-MW anions forming at high ratios due to oligomer degradation. Studies of an older Albemarle sample, however, indicated an increase in high-MW ions upon storage at room temperature. Our own aging studies confirm this, showing that MAO oligomers of low MW are slowly but systematically converted to those with higher MW at room temperature. This is the first observation of this process and contributes to the increased understanding of MAO. Additional computational investigations of the observed anions show large clusters with four-coordinate Al and three-coordinate O, which is in accordance with previous literature. All of these clusters have sites that can readily give up  $[\text{Me}_2\text{Al}]^+$  to form the observed  $[(\text{MeAlO})_x(\text{Me}_3\text{Al})_y\text{Me}]^-$  ions. It cannot, however, be excluded that the same species forms through  $\text{Me}^-$  abstraction, and a more detailed computational investigation to shed more light on this is ongoing. This work provides a clear insight into absolute MW, behavior, and interaction of discrete MAO oligomers. Future work will focus on the development of tools to investigate the neutral composition of MAO and further increase the understanding of this highly important activator.

Table 1. Anionization Potentials of Selected MAOs,  $(\text{MeAlO})_n(\text{Me}_3\text{Al})_m$ , Relative to the  $\text{Me}_3\text{Al}$  Dimer<sup>a</sup>

n	m	$(\text{MeAlO})_n(\text{Me}_3\text{Al})_m$	$[(\text{MeAlO})_x(\text{Me}_3\text{Al})_y\text{Me}]^-$ (x = n, y = m-1)	$\Delta E$ (kJ/mol)
16	7			-132.8
17	7			-170.5
18	7			-152.5
23	8			-155.4
26	8			-168.1

<sup>a</sup>Hydrogen atoms are omitted, and the  $[\text{Me}_2\text{Al}]^+$  group abstracted during ionization is highlighted for clarity (Al, pink; O, red; C, gray).

## EXPERIMENTAL SECTION

MAO (10 wt % in toluene) was purchased directly from Albemarle or received indirectly from NOVA Chemicals (stored 11 months at room temperature in a glovebox prior to shipping). Both samples were stored in the glovebox freezer upon receipt. The samples were warmed to room temperature and thoroughly swirled to dissolve any precipitated content prior to use.  $\text{Me}_3\text{Al}$  and  $[\text{Me}_2\text{Al}]^+$  concentrations of the MAO samples were determined following literature

procedures.<sup>5,16</sup> OMTS (98%) was purchased from Sigma-Aldrich and used as received. THF was dried using a MBraun SPS drying system and stored over activated molecular sieves. Fluorobenzene (Oakwood) was refluxed over  $\text{CaH}_2$ , distilled under  $\text{N}_2$ , and dried over molecular sieves inside a glovebox for at least 3 days prior to use.

**ESI-MS Details.** In a typical procedure a stock solution (3 mL) was prepared from 0.5 mL of MAO (1.5 M) and the amount of a PhF solution of OMTS (0.015 or 0.15 M) needed to give the desired OMTS:Al ratio. After mixing, 0.2 mL of this solution was further

diluted to a total volume of 3 mL ( $[Al] = 0.017\text{ M}$ ). This was injected from the glovebox into a Micromass QTOF *micro* spectrometer via PTFE tubing (1/16 in. o.d., 0.005 in. i.d.). The capillary voltage was set at 3000 V with source and desolvation gas temperatures at 85 and 185 °C, respectively, with a desolvation gas flow at 400 L/h. MS/MS data were obtained in product ion spectra using argon as the collision gas and a voltage range of 2–80 V.

**Computational Details.** Models for the neutral MAOs were produced by following the  $Me_3Al$  hydrolysis reactions, precisely by the procedure reported previously.<sup>8b,14b,19b</sup> The feasibility of anion formation via  $[Me_2Al]^+$  loss from the neutral MAOs was evaluated on the basis of relative anionization potentials, which are relative energies of the reaction  $MAO \rightarrow [Me_2Al]^+[MAO-Me]^-$ .<sup>16</sup> Association of  $Me_3Al$  into the MAO oligomers gives rise to dispersive interactions that complicate theoretical treatment of these molecules. The M06 series of functionals<sup>21</sup> has been recently shown as a cost-effective alternative for correlated ab initio methods in studies involving MAO.<sup>22</sup> The calculations were carried out at the M062X/TZVP level of theory<sup>23</sup> using Gaussian 09.<sup>24</sup> The neutral MAO molecules were confirmed as true local minima in the potential energy surface by calculation of harmonic vibrational frequencies.

## ■ ASSOCIATED CONTENT

### Supporting Information

The Supporting Information is available free of charge on the ACS Publications website at DOI: 10.1021/acs.organomet.7b00153.

Additional MS spectra and MSMS data (PDF)

Cartesian coordinates for the calculated structures (XYZ)

## ■ AUTHOR INFORMATION

### Corresponding Author

\*E-mail for J.S.M.: mcindoe@uvic.ca.

### ORCID

Harmen S. Zijlstra: 0000-0002-5754-5998

Mikko Linnolahti: 0000-0003-0056-2698

J. Scott McIndoe: 0000-0001-7073-5246

### Notes

The authors declare no competing financial interest.

## ■ ACKNOWLEDGMENTS

H.S.Z. and J.S.M. thank NOVA Chemicals' Centre for Applied Research for a kind donation of MAO, financial support, and useful discussions. J.S.M. thanks the NSERC (Strategic Project Grant # 478998-15) for operational funding and CFI, BCKDF, and the University of Victoria for infrastructural support. S.C. acknowledges support for a visiting scientist position from the University of Victoria. M.L. acknowledges support from the Academy of Finland (project no. 251448). The computations were made possible by use of the Finnish Grid Infrastructure and Finnish Grid and Cloud Infrastructure resources.

## ■ REFERENCES

- (1) Andresen, A.; Cordes, H. J.; Herwig, J.; Kaminsky, W.; Merck, A.; Mottweiler, R.; Pein, J.; Sinn, H.; Vollmer, H. J. *Angew. Chem., Int. Ed. Engl.* **1976**, *15*, 630–632.
- (2) Baier, M. C.; Zuideveld, M. A.; Mecking, S. *Angew. Chem., Int. Ed.* **2014**, *53*, 9722–9744.
- (3) For reviews on catalyst activation by MAO see: (a) Chen, E. Y. X.; Marks, T. J. *Chem. Rev.* **2000**, *100*, 1391–1434. (b) Bochmann, M. *J. Organomet. Chem.* **2004**, *689*, 3982–3998. (c) Bochmann, M. *Organometallics* **2010**, *29*, 4711–4740.
- (4) Zijlstra, H. S.; Harder, S. *Eur. J. Inorg. Chem.* **2015**, *2015*, 19–43 and references therein.

(5) Imhoff, D. W.; Simeral, L. S.; Sangokoya, S. A.; Peel, J. H. *Organometallics* **1998**, *17*, 1941–1945.

(6) (a) Babushkin, D. E.; Simikolenova, N. V.; Panchenko, V. N.; Sobolev, A. P.; Zakharov, V. A.; Talsi, E. P. *Macromol. Chem. Phys.* **1997**, *198*, 3845–3854. (b) Zakharov, V. A.; Talsi, E. P.; Zakharov, I. I.; Babushkin, D. E.; Semikolenova, N. V. *Kinet. Catal.* **1999**, *40*, 836–850. (c) Bryant, P. L.; Harwell, C. R.; Mrse, A. A.; Emery, E. F.; Gan, Z.; Caldwell, T.; Reyes, A. P.; Kuhns, P.; Hoyt, D. W.; Simeral, L. S.; Hall, R. W.; Butler, L. G. *J. Am. Chem. Soc.* **2001**, *123*, 12009–12017.

(7) (a) Von Lacroix, K.; Heitmann, B.; Sinn, H. *Macromol. Symp.* **1995**, *97*, 137–142. (b) Rocchigiani, L.; Busico, V.; Pastore, A.; Macchioni, A. *Dalton Trans.* **2013**, *42*, 9104–9111.

(8) See for example: (a) Zurek, E.; Ziegler, T. *Prog. Polym. Sci.* **2004**, *29*, 107–148. (b) Linnolahti, M.; Laine, A.; Pakkanen, T. A. *Chem. - Eur. J.* **2013**, *19*, 7133–7142. (c) Kuklin, M. S.; Hirvi, J. T.; Bochmann, M.; Linnolahti, M. *Organometallics* **2015**, *34*, 3586–3597.

(9) (a) Mason, M. R.; Smith, J. M.; Bott, S. G.; Barron, A. R. *J. Am. Chem. Soc.* **1993**, *115*, 4971–4984. (b) Harlan, C. J.; Mason, M. R.; Barron, A. R. *Organometallics* **1994**, *13*, 2957–2969. (c) Harlan, C. J.; Bott, S. G.; Barron, A. R. *J. Am. Chem. Soc.* **1995**, *117*, 6465–6474.

(10) (a) Santos, L. S.; Metzger, J. O. *Angew. Chem., Int. Ed.* **2006**, *45*, 977–981. (b) Jiang, J.; Zhang, H.; Li, M.; Dulay, M. T.; Ingram, A. J.; Li, N.; You, H.; Zare, R. N. *Anal. Chem.* **2015**, *87*, 8057–8062.

(11) Castro, P. M.; Lahtinen, P.; Axenov, K.; Viidanoja, J.; Kotiaho, T.; Leskelä, M.; Repo, T. *Organometallics* **2005**, *24*, 3664–3670.

(12) Lubben, A. T.; McIndoe, J. S.; Weller, A. S. *Organometallics* **2008**, *27*, 3303–3306.

(13) Henderson, M. A.; Trefz, T.; Collins, S.; McIndoe, J. S. *Organometallics* **2013**, *32*, 2079–2083.

(14) (a) Trefz, T. K.; Henderson, M. A.; Wang, M. Y.; Collins, S.; McIndoe, J. S. *Organometallics* **2013**, *32*, 3149–3152. (b) Trefz, T. K.; Henderson, M. A.; Linnolahti, M.; Collins, S.; McIndoe, J. S. *Chem. - Eur. J.* **2015**, *21*, 2980–2991.

(15) (a) Sangokoya, S. A. (Albemarle Corp.) PCT Int. WO 1998047929A1, 1999. (b) Sangokoya, S. A.; Goodall, B. L.; Simeral, L. S. (Albemarle Corp.) PCT Int. WO 03/082879, 2003. (c) Luo, L.; Sangokoya, S. A.; Wu, X.; Diefenbach, S. P.; Kneale, B. (Albemarle Corp.) US Patent Appl. 2009/0062492, 2009.

(16) Ghiotto, F.; Pateraki, C.; Tanskanen, J.; Severn, J. R.; Luehmann, N.; Kusmin, A.; Stellbrink, J.; Linnolahti, M.; Bochmann, M. *Organometallics* **2013**, *32*, 3354–3362.

(17) Henderson, M. A.; McIndoe, J. S. *Chem. Commun.* **2006**, 2872–2874.

(18) (a) Kaminsky, W.; Strübel, C. *J. Mol. Catal. A: Chem.* **1998**, *128*, 191–200. (b) Stellbrink, J.; Niu, A.; Allgauer, J.; Richter, D.; Koenig, B. W.; Hartmann, R.; Coates, G. W.; Fetters, L. J. *Macromolecules* **2007**, *40*, 4972–7981. (c) Zijlstra, H. S.; Harder, S. *Macromolecules* **2015**, *48*, 5116–5119.

(19) (a) Linnolahti, M.; Luhtanen, T. N. P.; Pakkanen, T. A. *Chem. - Eur. J.* **2004**, *10*, 5977–5987. (b) Hirvi, J. T.; Bochmann, M.; Severn, J. R.; Linnolahti, M. *ChemPhysChem* **2014**, *15*, 2732–2742.

(20) (a) Falls, Z.; Tymińska, N.; Zurek, E. *Macromolecules* **2014**, *47*, 8556–8569. (b) Tymińska, M.; Zurek, E. *ACS Catal.* **2015**, *5*, 6989–6998. (c) Falls, Z.; Zurek, E.; Autschbach, J. *Phys. Chem. Chem. Phys.* **2016**, *18*, 24106–24118.

(21) Zhao, Y.; Truhlar, D. G. *Theor. Chem. Acc.* **2008**, *120*, 215–241.

(22) (a) Boudene, Z.; De Bruin, T.; Toulhoat, H.; Raybaud, P. *Organometallics* **2012**, *31*, 8312–8322. (b) Ehm, C.; Antinucci, G.; Budzelaar, P. H. M.; Busico, V. *J. Organomet. Chem.* **2014**, *772–773*, 161–171.

(23) Schäfer, A.; Huber, C.; Ahlrichs, R. *J. Chem. Phys.* **1994**, *100*, 5829–5835.

(24) Frisch, M. J., et al. *Gaussian 09, Revision C.01*; Gaussian, Inc., Wallingford, CT, 2010.